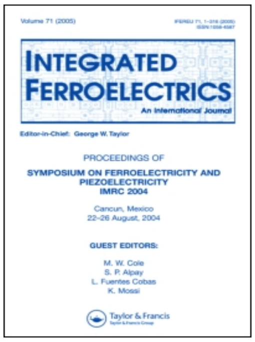

Integrated Ferroelectrics
An International Journal

ISSN: 1058-4587 (Print) 1607-8489 (Online) Journal homepage: http://www.tandfonline.com/loi/ginf20

Preparation and waveguiding properties of SOL-GEL derived lathanum modified lead titanate slab waveguides

Dae Sung Yoon , Junmo Koo , Seong Jin Kim , Byeong-Soo Bae , Won Jong Lee , Sang Hee Cho & Kwangsoo No

To cite this article: Dae Sung Yoon , Junmo Koo , Seong Jin Kim , Byeong-Soo Bae , Won Jong Lee , Sang Hee Cho & Kwangsoo No (1998) Preparation and waveguiding properties of SOL-GEL derived lathanum modified lead titanate slab waveguides, Integrated Ferroelectrics, 20:1-4, 141-158, DOI: 10.1080/10584589808238777

To link to this article: https://doi.org/10.1080/10584589808238777

Published online: 27 Sep 2006.

Submit your article to this journal

Article views: 15

Full Terms & Conditions of access and use can be found at
http://www.tandfonline.com/action/journalInformation?journalCode=ginf20

Integrated Ferroelectrics, 1998, Vol. 20, pp. 141 – 158
Reprints available directly from the publisher
Photocopying permitted by license only

© 1998 OPA (Overseas Publishers Association) N.V.
Published by license under
the Gordon and Breach Science
Publishers imprint.
Printed in India.

PREPARATION AND WAVEGUIDING PROPERTIES OF SOL-GEL DERIVED LATHANUM MODIFIED LEAD TITANATE SLAB WAVEGUIDES

DAE SUNG YOON[a,*], JUNMO KOO[b], SEONG JIN KIM[a], BYEONG-SOO BAE[b], WON JONG LEE[b], SANG HEE CHO[c] and KWANGSOO NO[b]

[a] *Micro-system Lab., Samsung Advanced Institute of Technology, PO Box 111, Suwon, Korea;*
[b] *Department of Materials Science and Engineering, Korea Advanced Institute of Science and Technology, Kusong-dong 373-1, Yusong-gu, Taejon 305-701, Korea;*
[c] *Department of Inorganic Materials Engineering, Kyungpook National University, Buk-gu, Taegu 702-701, Korea*

(Received 24 September 1996; In final form 17 December 1996)

Using sol-gel processing method, thin films of lathanum modified lead titanate (PLT) on Corning 7059 glass were prepared. Differential thermal analysis (DTA/TG) curve of gel powder and infrared spectra (FT-IR) of the films were measured to estimate proper heating schedule. Microstructures of the films were observed using a scanning electron microscope (SEM). The waveguiding properties and the propagation loss were measured using the prism coupling method. Effects of the drying conditions on the refractive indices and the propagation losses of the films were investigated. Experimental results showed that the grain size and the content of residual organics in the film decreased as the drying temperature of the film increased. As the drying temperature increased, the refractive index increased and the propagation loss decreased.

Keywords: PLT thin film; sol-gel; waveguide; prism coupling; propagation loss

1. INTRODUCTION

Recent years have brought renewed interest in integrated-optical applications of ferroelectric thin films.[1-5] The ferroelectric films have

*Corresponding author.

several potential advantages for electro-optic and nonlinear optical applications over the standard technology using diffused and ion exchanged waveguides in single crystal materials such as lithium niobate and lithium tantalate. These potential advantages include compatibility with a variety of substrates, low processing temperatures, easy manufacture at low cost and capability of deposition over large area. On the other hand, fabricating the films of good enough optical quality to permit waveguiding over long distance has proved to be difficult.

There have been many recent advances in the technology of deposition of thin films of lanthanum modified lead titanate (PLT) and related ferroelectric films. The ferroelectric PLT films exhibit both excellent transparency and strong elector-optic effects. A few researchers have tried to fabricate the PLT thin films for the waveguide application using the sputtering method.[6–9] The propagation losses of the sputter-deposited PLT film, however, are too high (approximately $5 \sim 15$ dB/cm), which is possibly due to the larger grain size by using the high deposition temperature. The degree of homogeneity of sputter-deposited films is lower than that of solution derived films. Recently, Teowee [10] reported that the small grain size of the crystalline film inherent in the low temperature sol-gel processing contributes to the low propagation loss of < 3 dB/cm for PLT film.

Using sol-gel processing method, we have prepared PLT films having excellent optical quality on Corning 7059 glass substrates. It was found that the drying conditions during the film preparation critically affects the propagation losses of the films. These films are of suitable thickness to permit optical waveguiding of visible light. In this paper, the preparation method and the waveguide property measurements of PLT films on Corning 7059 glass substrates were described. The drying temperature dependence of the refractive indices and the propagation losses in the films will be discussed.

2. EXPERIMENTAL PROCEDURE

Preparation of PLT Thin Film

A flow diagram for preparation of PLT films is shown in Figure 1. The precursors for the PLT solutions were lead acetate trihydrate,

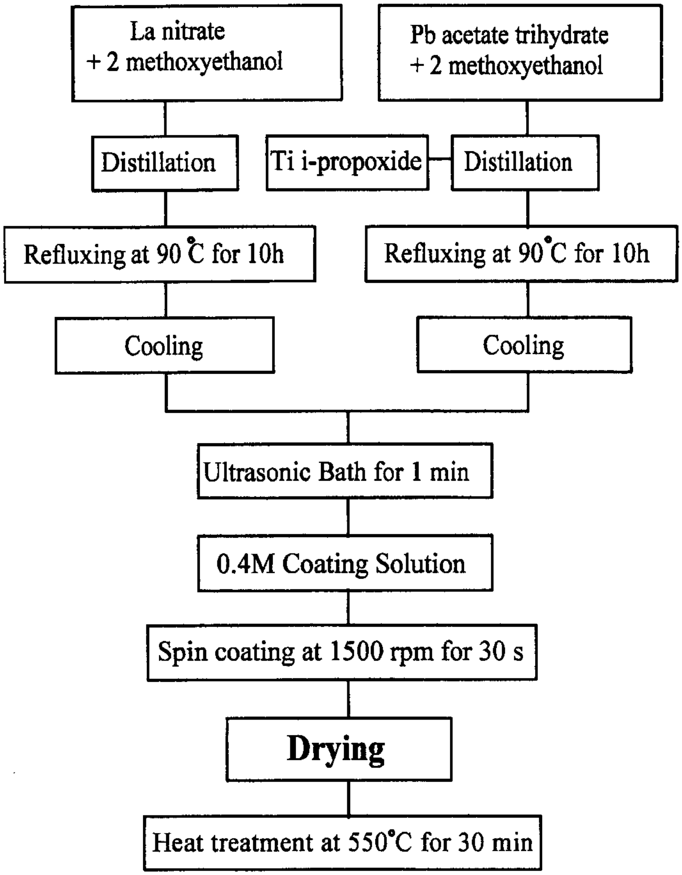

FIGURE 1 A Flow diagram for preparation of the PLT films.

lanthanum nitrate and titanium iso-propoxide. Lead acetate trihydrate was dissolved in methoxyethanol, and the solution was distilled to remove water associated with the lead acetate precursor. Titanium iso-propoxide pre-dissolved in methoxyethanol were added to the lead methoxyethanol solution. The solution mixture was distilled to a final concentration of about 0.4 M and then refluxed. For the preparation of a lanthanum nitrate solution, lanthanum nitrate was also dissolved in methoxyethanol, and the solution was distilled for 1 h and then refluxed. A coating solution for the film preparation was fabricated by mixing an equal volume of two solutions. The films were deposited using the spin-coating onto Corning 7059 glass substrates at 1200 rpm for 30 sec. The deposition process involved multiple cycles of the spin coating followed by intermediate drying process. The PLT films were dried at 350°C, 400°C, 450°C and 500°C. The drying time was 30 minutes. The drying processes of the films were conducted on a hot plate. Each spin coating and drying cycle contributed an average film thickness of about 0.11 μm. The coating and the drying procedures were iterated 5 times to obtain the desired film thickness of about $0.5 \sim 0.6$ μm. After the coating and the drying procedures, all of the fabricated PLT films were heat-treated at 550°C for 30 min under air atmosphere in a furnace. DTA/TG curve of gel powder and FT-IR spectra of the films were measured to estimate residual organics in them. Microstructures of the films were observed with a scanning electron microscope.

Prism Coupling Set-up

The experimental arrangement for the observation of the coupling and for the measurement of the coupling angle is shown schematically in Figure 2(a). The film under test is pressed against the base of a coupled prism using a micrometer. A right-angle prism made of rutile was used for coupling. Because the rutile prism is a uniaxial birefringent crystal, the optical axis should be oriented parallel to the 45° edge plane of the prism. This orientation allows us to obtain a constant prism index n_p, which is the ordinary index for TE polarization, and the extraordinary index for TM polarization. A lens focuses the beam into the prism so that the beam waist coincides with the prism base.

Calculation of Effective Index and Refractive Index

Besides the prism shape, the most important parameters of a coupling prism are its refractive index n_p and the prism angle ε. They determine the range of the effective index, $N = n_p \sin\theta$ of the light along the prism base, which is related to the incidence angle at the entrance face of the prism. We are able to determine the effective index of the

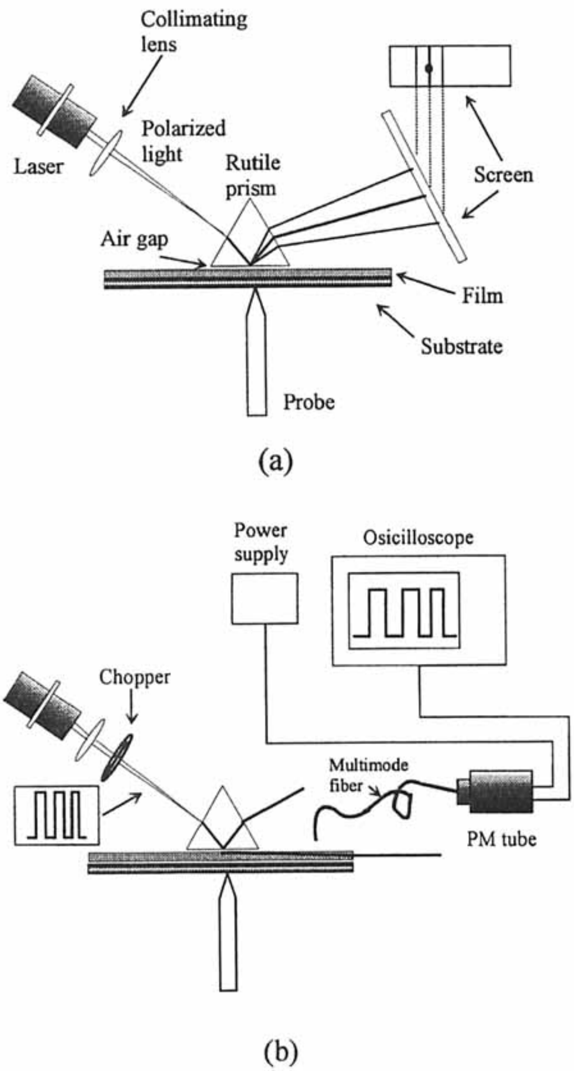

FIGURE 2 Experimental set-up for (a) the measurement of the coupling angle and the mode observation, and (b) the measurement of the propagation losses.

corresponding modes with respect to the input angle using the Snells law by

$$N = \sin\alpha\cos\varepsilon + (n_p^2 - \sin^2\alpha)^{1/2}\sin\varepsilon \qquad (1)$$

The results of the measurements are a list containing the observed modes of the film, identified by their mode numbers $m = 0, 1, 2, \ldots$, and for each mode the measured coupling angle α_m. The observed effective indices $N_0, N_1, \ldots$ are related to the unknown n and W by the dispersion equation [11] of the planar dielectric waveguide.

$$kT = (m+1)\pi - \tan(k_x/\gamma_s) - \tan(k_x/\gamma_c) \tag{2}$$

where $\gamma_c = k_0(N^2 - n_c^2)^{1/2}$, $\gamma_s = k_0(N^2 - n_s^2)^{1/2}$, $k_x = k_0(n_f^2 - N^2)^{1/2}$, and T is the film thickness. When we solved the equations corresponding to each mode, the refractive index of the film were calculated from the known mode angles.

Propagation Loss

Successful waveguiding over the specimens with the length of about 2 cm was established. The brightness of a guided wave streak (*i.e.*, the scattered light intensity) is proportional to the guided light intensity at each point, provided that the waveguide is uniform. The measurement of the propagation loss in each of the films was conducted using the scattering detection method [Fig. 2(b)].[12] The propagation losses of the films were obtained from the following equation:

$$\alpha = |\,10\log(P_1/P_2)/(L_1 - L_2)| \tag{3}$$

where L_1 and L_2 are the distances from the coupling place, and P_1 and P_2 are the intensities of the scattered beams, respectively.

3. RESULTS AND DISCUSSION

To estimate the thermal decomposition characteristics of the PLT gel powder, DTA/TG curves of the gel powder with 20 at.% La were measured under a heating rate of 5 °C/min and in air atmosphere. Figure 3 shows DTA/TG curves of the dry gel of the PLT coating solution. Three exothermic peaks at 200°C, 280°C and 490°C are observed. The peak at 200°C and 280°C are attributed to the decomposition of the metal organic compound and the formation of CO_2 and H_2O. The peak at around 490°C is attributed to the

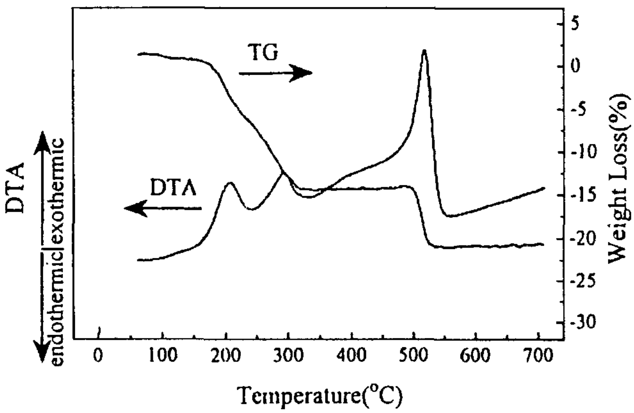

FIGURE 3 DTA/TG curves of PLT dry gel.

decomposition of the residual organics and possible crystallization of the amorphous film. However, the precise crystallization temperature cannot be determined because the crystallization peak is embedded into the decomposition peak of the residual organics. In the case of the TG curve, first weight loss of the gel powder occurs between 200°C and 280°C. Second weight loss of the gel powder occurs drastically at the temperature of around 500°C. However, the weight loss of the gel powder remains constant in the temperature region between 300°C and 490°C. That trend of the gel powder is quite different from the following FT-IR spectra of the PLT thin films dried at various drying temperatures.

Figure 4 shows the FT-IR spectra of the PLT thin films dried at different temperatures. Many absorption peaks due to various chemical bonds such as CH_3, CH, COO, H–OH and CO are observed in the case of the gel film which was dried at 80°C on a hotplate. The film dried at 300°C shows the absorption peak due to CO, COO and H–OH bond. As the drying temperature increase, the peak intensities of CO, COO and H–OH bonds decrease gradually. At the temperature above 400°C, the samples show the absorption peaks of CO_2 which was trapped in the films due to burning-out. The residual organics and the trapped CO_2 may give rise to the formation of micropores which lead the decrease of the density and of the refractive index. From above result, it is known that the residual organics in the

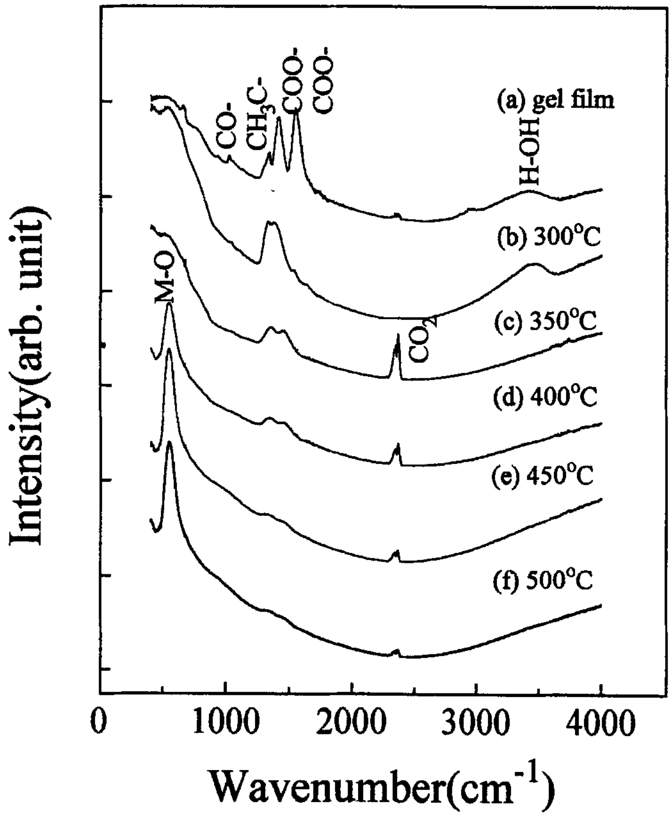

FIGURE 4 FT-IR spectra of the PLT films dried at different temperatures.

film decrease gradually in the temperature region between 300°C and 500°C, which is different from the observations made in DTA/TG curves of the gel powder.

The phase and the crystal orientation of the films were characterized using X-ray diffraction analysis. Figure 5 shows XRD patterns of the films with various La contents. In all cases, the films mainly consist of perovskite phase, and pyrochlore phase is not observed within a resolution limit of the XRD. The XRD patterns of all PLT films show no significant (h00) and (001) peak split, which may indicate that the phase is not tetragonal. The observed discrepancy in the peak split between the bulk and the film may be due to the thermal history and/

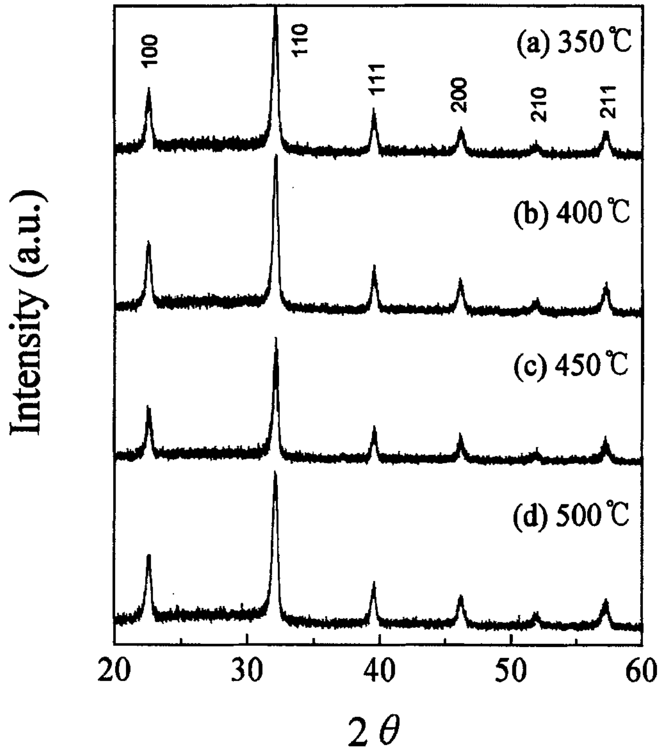

FIGURE 5 X-ray diffraction patterns of the PLT film dried at different temperatures and fired at 550°C for 30 min.

or the substrate used in the sol-gel process. All films shows the random crystal orientation, which is due to the substrate (Corning glass).

Figure 6 shows AFM images of the microstructures of the PLT films dried at different temperatures. The film dried at 350°C shows the large grain size of about 1 μm and seems to have relatively rough surface. The height difference (△) between the highest part and the lowest part in the film images is 9 nm. Much residual organics in that film may prohibit the formation of perovskite nuclei and lead the large grain structure. As the drying temperature increased, the grain size became smaller and the film surface smoother. The films dried at 400°C and 450°C have the height differences of about 4 ~ 5 nm. However, the film dried at 500°C consists of small and rough

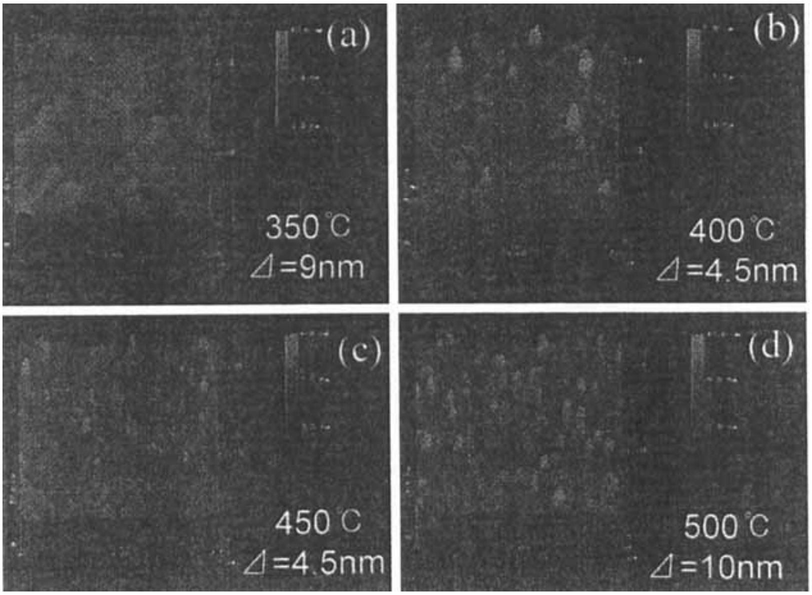

FIGURE 6 AFM images of PLT films dried at (a) 350°C, (b) 400°C, (c) 450°C and (d) 500°C, respectively, and fired at 550°C for 30 min.

perovskite grains which show $\triangle = 10$ nm. This may be due to that the combustion of organics and the crystallization of the films occur simultaneously at 500°C on the drying process. It is apparent that these microstructures affect the propagation losses of the films.

Ferroelectric properties of the films were measured using an RT66A ferroelectric test system (Radient Technology Co.) Figure 7 shows *P-E* hysteresis curves of the PLT films dried at different drying temperatures. Although the peak split between (h00) and (001) was not observed, all films show weak ferroelectricity in *P-E* hysteresis curves. As the drying temperature increased, the saturation polarization (P_s), the remanent polarization (P_r) and the coercive field(E_c) of the film increased. The film dried at 500°C have a saturation polarization of 39.7 $\mu C/cm^2$, a remanent polarization of 18.6 $\mu C/cm^2$ and a coercive field of 98 kV/cm.

Figure 8 shows the transmittance spectra of the PLT films fabricated at different drying temperatures for 30 min. The average transmittance

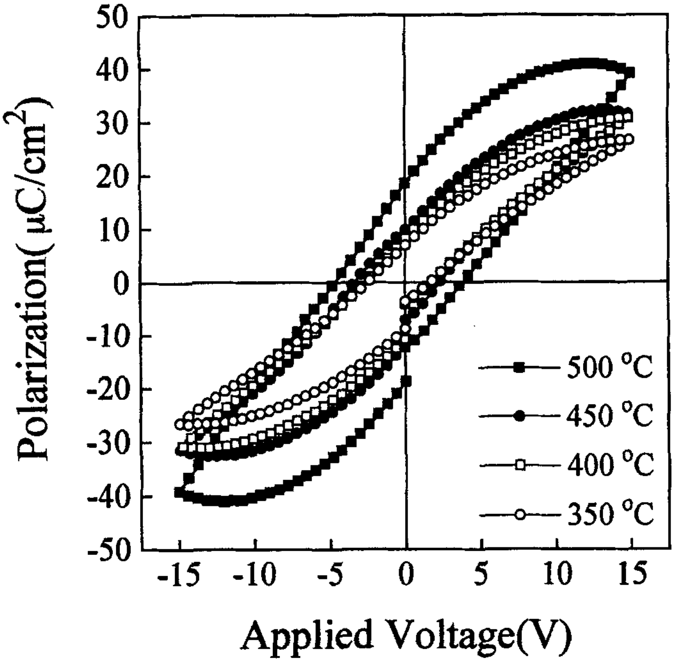

FIGURE 7 *P-E* hysteresis curves of the PLT films dried at different temperatures and fired at 550°C for 30 min.

of the film increased as the drying temperature increased. The observed average transmittance trend may be associated with the residual organics and the film density. The solvent in the film is evaporated at the drying temperature. However, the residual organics in the film does not burn out completely at the drying temperature. These residual organics remain accumulated in the film throughout the repeated coating and drying process and, then, are burned out in the final heat treatment. Some of the residual organics may serve as source of voids and micropores in the final film after the film is finally heat-treated. The voids and the micropores serves as source of light scattering, so that denser film (with higher drying temperature) may show higher transmittance.

The prism coupling method utilizes a high-index prism to excite a guided wave through the phase matching between the incident wave

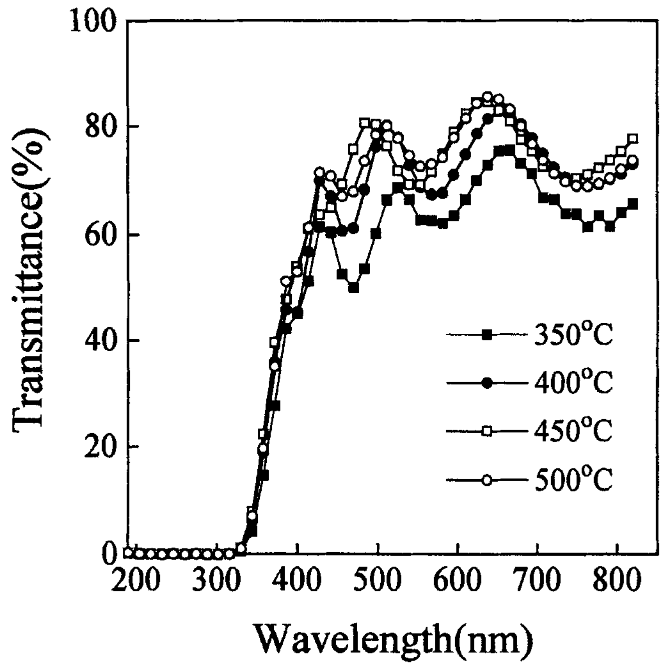

FIGURE 8 Transmittance spectra of the PLT films dried at different temperatures and fired at 550°C for 30 min.

and a guided wave. The effective index N along the waveguide plane depends on the incident angle, the prism index and the prism angle. In our system, the effective index N is expressed by

$$N = 0.7071 \times \{\sin\alpha + (2.584^2 + \sin^2\alpha)^{1/2}\} \tag{4}$$

Figure 9 shows the allowed effective index range in our system under the given prism (α = 45°C, n_p = 2.584). The effective indices are 1.46 and 2.43 for the incident angles of $-4/\pi$ and $+4/\pi$, respectively. As the incident angle increases, the effective index increases monotonously.

When the film was turned into any one of the synchronous directions under the incidence of laser beam, three phenomena were observed. : First, the intensity of the reflected spot was reduced. Figure 10 shows reflected beam intensity *vs.* incident angle characteristics of the 5 cycle coated PLT film dried at 450°C for 30 min. When a

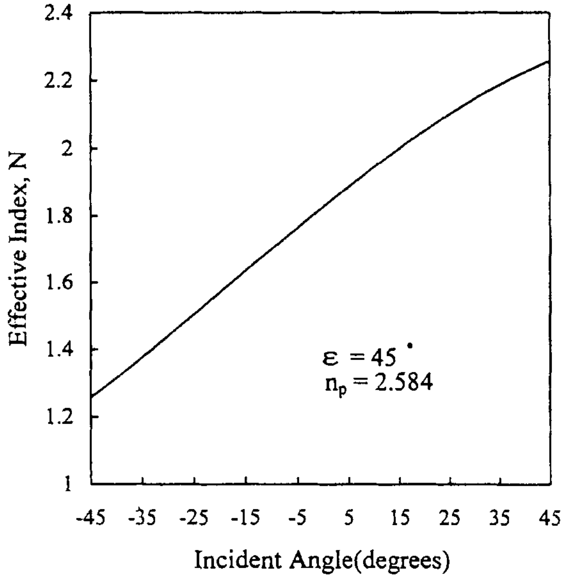

FIGURE 9 Allowed range of the effective indices in our system.

guided mode was excited, the intensity at the detector dropped abruptly. Three guided modes of TE_0, $TE_1$and TE_2 were excited in the film. As the coating cycle increased, the number of the observed guided modes increased. From the beam input angle at which guided modes occurred and the given properties of the prism, the guided-wave index was readily calculated. TE-polarized input light was used for the measurements, as in some cases not all TM modes could be excited with the available prism. Second, a small area of the film near the coupling spot appears very bright. Third, the bright m-line appeared on the screen only when the laser beam was coupled into a mode of the film. Figure 11 shows the bright *m*-line images of the 6 cycle coated PLT thin film dried at 450°C for 30 min. The light propagating in that mode was scattered into other directions (in the plane of the film) of the same mode and produced the bright lines on the screen. In accordance with this explanation it is characteristics for the bright *m*-lines that they all light up simultaneously when, during rotation of the prism, one of the coupling direction α_m passes through the direction of the input beam. Moreover, in each of these coupling situations, the reflected beam on the screen coincides with one of the *m*-lines.

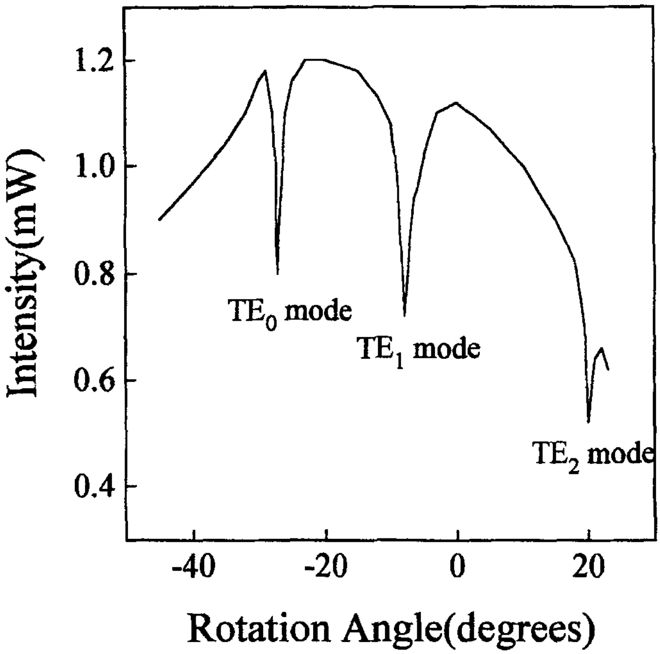

FIGURE 10 Reflected beam intensity *vs* incident angle characteristics of a PLT films with 6 cycles.

The refractive indices of the films were calculated from the mode angles. The calculation assumes that the samples consisted of homogeneous isotropic films on homogeneous isotropic substrates. Figure 12 shows the refractive indices of the films dried at different temperatures. The film dried at 350°C shows the refractive index of 2.305. As the drying temperature increases, the refractive index increases in spite of Pb loss at high temperature. This may indicate that residual organics lead the formation of micropores which may take a role in the decrease of the film density and the refractive index.

The propagation losses of the PLT films were measured using the scattering detection method. The measurement of the scattered light intensity distribution along the propagation of a guided wave therefore enables the determination of the propagation losses. It is found that the drying temperature strongly affects the propagation losses of the films. Figure 13 shows propagation losses of the PLT

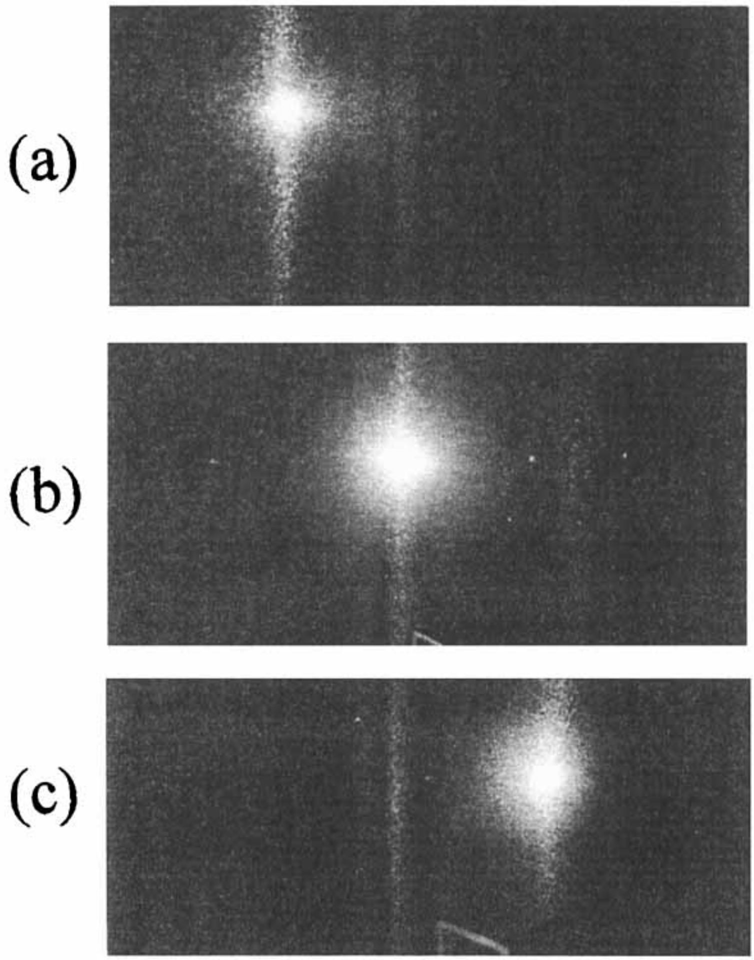

FIGURE 11 Bright *m*-line images of a PLT film with 6 coating cycles.

films dried at different temperatures. The film dried at 350°C has the propagation loss of 8.7 dB/cm. As the drying temperature increases, propagation loss of the film decreases. The film dried at 450°C shows the minimum propagation loss of 3.3 dB/cm. However, the film dried at 500°C have higher propagation loss (4.5 dB/cm) than that of the film dried at 450°C. It is apparent that rough surface in the film prohibits the light propagation and leads the increase of the

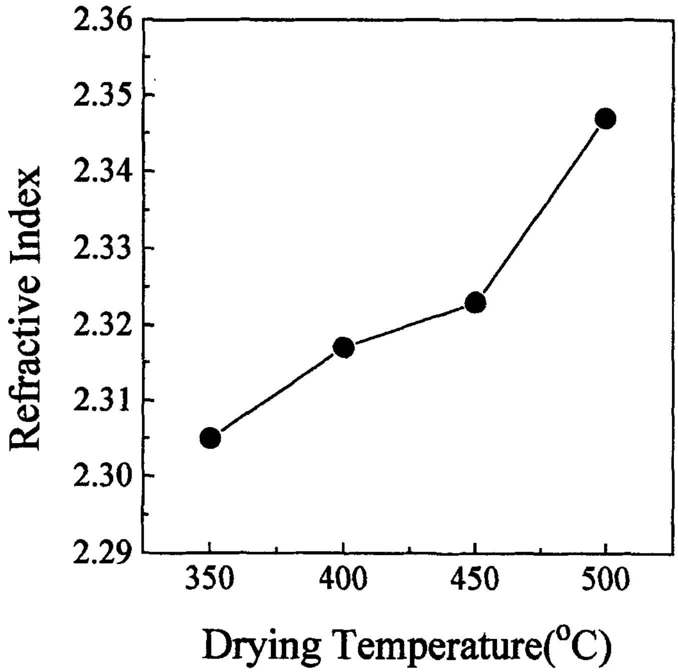

FIGURE 12 Refractive indices of PLT films dried at different temperatures and fired at 550°C for 30 min.

propagation loss. From above results, it may be speculated that the drying temperature dependence of the propagation losses is due to their microstructures and the residual organics in the films.

4. SUMMARY

Lanthanum modified lead titanate thin films were successfully fabricated using sol-gel method. The waveguiding properties and propagation loss were measured using the prism coupling method. Successful waveguiding was established in all the films. Effects of the drying conditions on the refractive indices and the propagation losses of the films were investigated. Experimental results showed that the grain size and the content of residual organics in the film decreased as

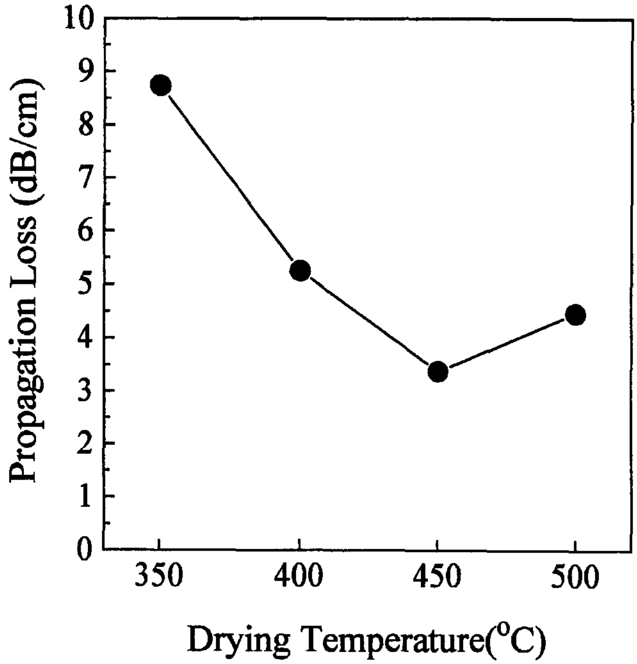

FIGURE 13 Propagation losses of PLT films dried at different temperatures and fired at 550°C for 30 min.

the drying temperature of the film increased. As the drying temperature increased, the refractive index increased and the propagation loss decreased.

Acknowledgment

The authors sincerely appreciate the financial support from KOSEF (Funding No. : 94-0300-06-01-3)

References

[1] Takayama, T., Shimizu, M. and Shiosaki, T. (1993). *Jpn. J. Appl. Phys.*, **32**, 3943.
[2] Fox, G. R. and Krupanidhi, S. B. (1993). *J. Appl. Phys.*, **74**(3), 1949.
[3] Baude, P. F., Ye, C., Tamagawa, T. and Polla, D. L. (1993). *J. Appl. Phys.*, **73**, 7960.
[4] Wood, V. E., Busch, J. R., Ramamurthi, S. D. and Swartz, S. L. (1992). *J. Appl. Phys.*, **71**(9), 4557.

[5] Kaminow, I. P. and Stulz, L. W. (1978). *Appl. Phys. Lett.*, **33**(1), 62.
[6] Tawaguchi, T., Adachi, H., Setsune, K., Yamazaki, O. and Wasa, K. (1984). *Appl. Opt.*, **21**(13), 2187.
[7] Adachi, H., Kawaguchi, T., Setsune, K., Ohji, K. and Wasa, K. (1983). *Appl. Phys. Lett.*, **42**, 867.
[8] Adachi, H., Mitsuyu, T., Yamazaki, O. and Wasa, K. (1986). *J. Appl. Phys.*, **60**, 736.
[9] Wagner, A. B., Brueck, S. R. J. and Wu, A. Y. (1991). *Ferroelectrics*, **116**, 195.
[10] Teowee, G., Baertlein, C. D., Quackenbush, E. L., Motakef, S., Boulton, J. M. and Uhlmann, D. R. (1994). *SPIE Proc.*, **2288**, 599.
[11] Ulrich, R. and Torge, R. (1973). *Appl. Opt.*, **12**(12), 2901.
[12] Goell, J. E. and Standley, R. D. (1969). *Bell Syst. Tech. J.*, **48**(10) 3445.